

# Monofluorination and Trifluoromethylation of BODIPY Dyes for Prolonged Single-Molecule Detection\*\*

Anh Minh Huynh,<sup>[a]</sup> Johannes Menges,<sup>[a]</sup> Michael Vester,<sup>[a]</sup> Tobias Dier,<sup>[b]</sup> Volker Huch,<sup>[c]</sup> Dietrich A. Volmer,<sup>[b]</sup> and Gregor Jung<sup>\*[a]</sup>

Electrophilic monofluorination with Selectfluor and nucleophilic trifluoromethylation with the Ruppert–Prakesh reagent of dimethyl-, tetramethyl- and pentamethyl-substituted boron dipyrromethenes (BODIPY) are investigated. Monofluorinated dyes are synthesized with low yields (<30%), however trifluoromethyl derivatives are obtained in moderate to high yields ( $\approx$ 40–90%). All compounds are characterized by steady-state and time-resolved fluorescence spectroscopy, the photostability is investigated with fluorescence correlation spectroscopy

(FCS) and total internal reflection fluorescence microscopy (TIRF). Monofluorination hardly affects the spectroscopic parameters of the unsubstituted parent compounds, but distinctly enhances the photostability, whereas trifluoromethylation leads to a hypsochromic shift by up to 17 nm in both absorption and emission, slightly enhanced intersystem crossing, and higher photostability. Further development of soft fluorination and trifluoromethylation methods is therefore highly desired.

## 1. Introduction

Fluorine is known as the most electronegative element in the periodic table of elements and the C–F bond is one of the strongest single bonds. As  $^{19}\text{F}$  is the only natural isotope of fluorine, it is convenient for nuclear magnetic resonance (NMR) characterization.<sup>[1]</sup> For example, fluorinated amino acids have been incorporated into fluorescent proteins such as enhanced green fluorescent protein (EGFP), enhanced yellow fluorescent protein (EYFP), and cyan fluorescent protein (CFP).<sup>[2]</sup> NMR analysis allows the study of the thermodynamics of conformational changes. Additionally, the easy introduction of a fluorine atom, that is, the isotope  $^{18}\text{F}$ , in a molecule also enables the use of positron emission tomography (PET).<sup>[3]</sup> Furthermore, organofluorine substituents such as trifluoromethyl ( $\text{CF}_3$ ) also affect intermolecular interactions<sup>[4]</sup> and are therefore used to adjust molecular physical properties, for example in liquid crystals.<sup>[5]</sup> They also find applications in magnetic resonance imaging (MRI).<sup>[6]</sup> As fluorine and trifluoromethyl substituents can also enhance pharmacokinetic properties,<sup>[7]</sup> these groups are often used to replace hydrogen atoms in bioactive target molecules. Besides their widespread applications in life science and medi-

cal chemistry, such substitutions can increase the intrinsic photostability of fluorophores such as triarylmethane, xanthone, and rhodamine dyes.<sup>[8]</sup>

This latter point provoked our interest, as the presence of stabilizers<sup>[9]</sup> may interfere with our long-term goal of single-molecule chemistry.<sup>[11]</sup> Boron dipyrromethene (**1**; BODIPY, Figure 1) dyes are good fluorophores as a starting point for improvement.<sup>[10]</sup> They have narrow excitation and emission bands, high quantum yields, and are more photostable than fluorescein dyes.<sup>[11]</sup> Consequently, BODIPY dyes are enormously popular and have versatile uses as fluorescent switches, laser dyes, biomolecule markers, and chemosensors.<sup>[10a,b,12]</sup> Despite plenty of applications and many ways to modify the BODIPY core, at the moment hardly any attempts have been made to intrinsically improve the photophysical properties of BODIPY dyes with fluorine and trifluoromethylated substituents. Yet described derivatives are often trifluoromethylated at the 8-position (meso position) of the BODIPY core (Figure 1).<sup>[13]</sup> A general method to synthesize these dyes is the reaction between trifluoroacetaldehyde methyl hemiacetal and pyrrole.<sup>[13b]</sup> In a recent publication, radical trifluoromethylation at the 3-position ( $\alpha$  position, Figure 1) of a symmetrical BODIPY dye is described.<sup>[14]</sup> However, the spectroscopic effects of F and  $\text{CF}_3$  substituents on the fluorophores are still unknown, especially their influence on the photostability.

As we are especially interested in following chemical reactions by ultrasensitive fluorescence methods,<sup>[1,15]</sup> high photostability is mandatory for continuous observation. For further improvements, we therefore explored the modification of the BODIPY cores **2**, **3**, and **4** (Figure 1) at positions 3 and 2 ( $\alpha$  and  $\beta$ ) by using Selectfluor and the Ruppert–Prakash reagent. After monofluorination and trifluoromethylation, we examined the spectroscopic properties of the newly synthesized dyes **5–10**

[a] A. M. Huynh, J. Menges, M. Vester, Prof. Dr. G. Jung  
Biophysical Chemistry, Saarland University  
Campus Building B22, 66123 Saarbrücken (Germany)  
E-mail: g.jung@mx.uni-saarland.de

[b] T. Dier, Prof. Dr. D. A. Volmer  
Institute of Bioanalytical Chemistry, Saarland University  
66123 Saarbrücken (Germany)

[c] Dr. V. Huch  
Inorganic and General Chemistry, Saarland University  
66123 Saarbrücken (Germany)

[\*\*] BODIPY = boron dipyrromethenes

Supporting Information for this article is available on the WWW under <http://dx.doi.org/10.1002/cphc.201500869>.

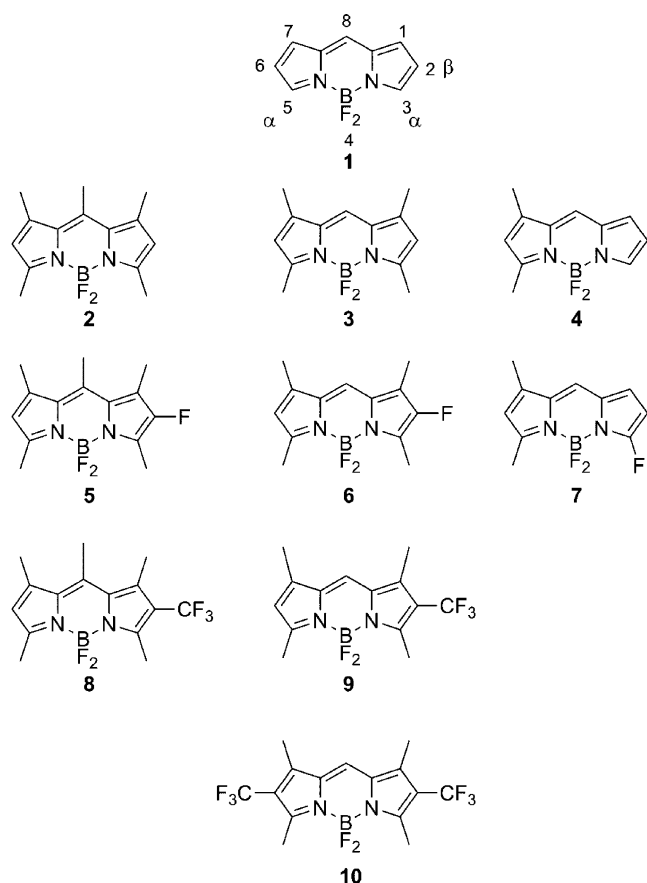


Figure 1. Basic BODIPY framework (1) and synthesized derivatives 2–10.

and compared their photostability with the parent compounds by using fluorescence correlation spectroscopy (FCS) and total internal reflection fluorescence microscopy (TIRF).

## 2. Results and Discussion

### 2.1 Synthesis

In the past 20 years electrophilic fluorination and nucleophilic trifluoromethylation have been thoroughly explored.<sup>[16]</sup> The introduction of a fluorine atom or a trifluoromethyl substituent into a BODIPY dye at specific locations can be achieved through several methods. Reagents used to form a C–F bond are commercially available. Noteworthy nucleophilic reagents are diethylaminosulfur trifluoride (DAST),<sup>[17]</sup> 2,2-difluoro-1,3-dimethylimidazolidine (DFI),<sup>[18]</sup> and bis(2-methoxyethyl)amino-sulfur trifluoride (Deoxofluor).<sup>[19]</sup> Special equipment for handling these compounds is required, thus limiting their widespread application. Electrophilic reagents consist of  $R_2N-F$  or  $R_3N^+-F$  units, for example the so-called Olah's reagent.<sup>[20]</sup> Since the discovery of Olah's reagent, a number of appropriate reagents were developed, for example *N*-fluorobenzene sulfonimide **11** (NFSI) and 1-chloromethyl-4-fluorodiazoniabicyclo[2,2,2]octane bis(tetrafluoroborate) **12** (Selectfluor I; Figure 2).<sup>[20]</sup>

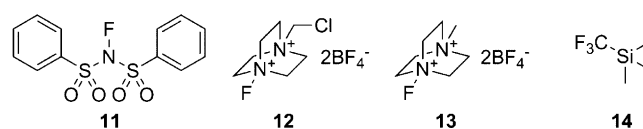


Figure 2. Electrophilic fluorination agents **11–13** and the Ruppert–Prakash reagent (**14**).

Trifluoromethyl substituents are usually introduced by nucleophilic substitution with trimethyl(trifluoromethyl) silane **14** (Ruppert–Prakash reagent)<sup>[19,21]</sup> or trifluoroacetamides.<sup>[20,22]</sup> For the electrophilic trifluoromethylation, there is a variety of reagents, with Togni's reagent being the most prominent one. This hypervalent-iodine-containing compound has already been used to synthesize a trifluoromethylated BODIPY dye in moderate yields.<sup>[14,23]</sup>

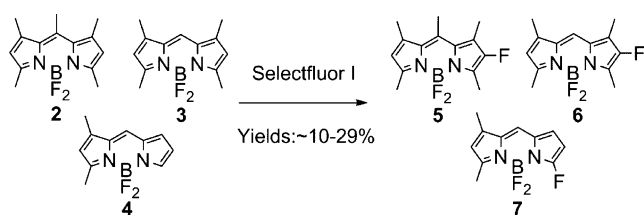
On the basis of the available knowledge, we envisaged the syntheses of various fluorinated and trifluoromethylated BODIPY dyes. Although fluorinated and trifluoromethylated pyrroles might be conceived as BODIPY building blocks, our attempts in this direction resulted in yields of under 3%. We therefore focused on derivatizing already formed dyes, as this protocol can also be applied to other BODIPY dyes with differing substitution patterns (Schemes 1–3).<sup>[11]</sup> There are two convenient possibilities to derivatize BODIPY dyes. The first and most straightforward way relies on direct electrophilic fluorination. Alternatively, halogenation, subsequent conversion into a boronic acid pinacol ester,<sup>[24]</sup> and finally, Pd-catalyzed insertion of fluorine by using electrophilic fluorination reagents<sup>[25]</sup> should also yield monofluorinated BODIPY dyes. The introduction of  $CF_3$  moieties also involves halogenated BODIPY frames as substrates for nucleophilic substitution.<sup>[26]</sup>

The outcome of the fluorination of the BODIPY dyes **2–4** with Selectfluor I is summarized in Table 1 (Scheme 1). The use of the standard conditions for monofluorination of aromatic

Table 1. Yields of electrophilic monofluorination of different BODIPY dyes (Scheme 1).

| Educt | Product | Solvent | Temperature [°C] | Yield [%] |
|-------|---------|---------|------------------|-----------|
| 4     | 7       | MeOH    | 25               | 2         |
| 4     | 7       | MeCN    | 90               | 29        |
| 3     | 6       | MeOH    | 25               | 3         |
| 3     | 6       | MeOH    | 60               | 10        |
| 2     | 5       | MeOH    | 25               | 4         |
| 2     | 5       | MeOH    | 60               | 12        |

compounds,<sup>[27]</sup> resulted in disappointingly low yields (7–15%). Subsequently, the conditions of the reaction were carefully improved (Table 1 and Table S1 in the Supporting Information). We found that the best conditions differed from compound to compound. The highest yield for the monofluorinated dimethyl BODIPY (**7**) was accomplished with Selectfluor I (**12**) in acetonitrile (MeCN) at 90 °C for 6 h. In contrast, the best reaction conditions for the synthesis of monofluorinated compounds **5** and **6** are Selectfluor I (**12**) in MeOH at 60 °C for 4 h. In all cases, the yield of the intended product was below 30%.



**Scheme 1.** Direct fluorination of BODIPY dyes.

Upon using higher temperatures for converting compounds **2** and **3**, we observed a purple-colored reaction mixture, especially when using Selectfluor II (**13**) and NFSI (**11**), from which an orange fluorescent compound could be isolated ( $\lambda_{\text{ex}} = 553$ ,  $\lambda_{\text{em}} = 574$  nm). A comparison with published mass spectrometric data<sup>[28]</sup> unambiguously revealed the formation of trimeric BODIPY,<sup>[29]</sup> presumably as a result of a single-electron transfer (SET).<sup>[27-29]</sup> Interestingly, the higher yield of **7** compared with that of **5** and **6**, the reaction conditions, and the regioselectivity are in full agreement with the recently described introduction of chlorine at the  $\alpha$  position.<sup>[30]</sup> There, a cationic radical is postulated as an intermediate, which is formed through SET as well, whereas regular electrophilic halogenation of the BODIPY scaffold favors the  $\beta$  carbon atom.<sup>[31]</sup> The formation of **5** and **6**, therefore, can only be achieved when the  $\alpha$  position is blocked, but then in distinctly lower yields than with other halogens.

Owing to the low yields, we considered synthesizing fluorinated dyes through an indirect route (Scheme 2). The brominated BODIPY dyes **17**, **20**, and **21** were synthesized according to existing procedures.<sup>[15b,24]</sup> These halogenated compounds were transformed into the pinacol esters **22**, **23**, and **24**, through reaction with bis(pinacolato)diboron,  $\text{K}_2\text{CO}_3$ , and  $[\text{Pd}(\text{dppf})\text{Cl}_2]$  [ $\text{dppf} = 1,1'$ -bis(diphenylphosphino)ferrocene] in THF at  $90^\circ\text{C}$  (yields  $\approx 16$ – $33\%$ ). We then followed a recently

published method<sup>[25]</sup> to substitute the pinacol ester in a Pd-catalyzed reaction with Selectfluor I (**12**), as the fluorine source, in MeCN at  $40^\circ\text{C}$ . Unfortunately, the yields of **5**–**7** were below those of the direct electrophilic fluorination (1–2% over three steps). However, enough material could be collected from the syntheses for a thorough characterization including X-ray crystallography (Figure 3). The analysis revealed the expected structures with  $\text{BF}_2$  moieties perpendicular to the dipyrromethene core.

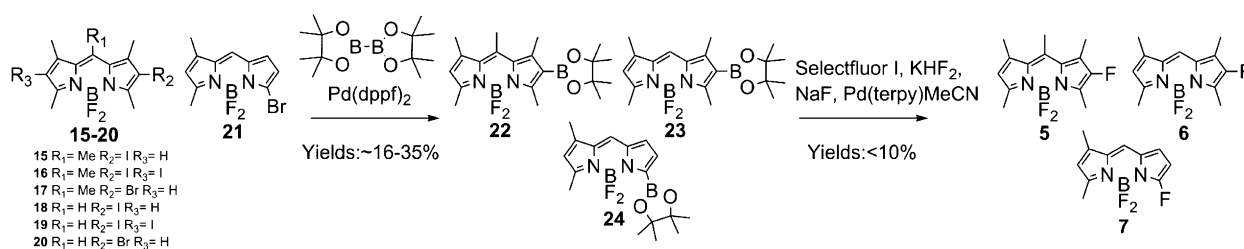
Trifluoromethylated BODIPY dyes were synthesized starting from the halogenated core (Table 2). According to a method

**Table 2.** Yields of halogenation pathway for monofluorinated and trifluoromethylation BODIPY dyes (Schemes 2 and 3).

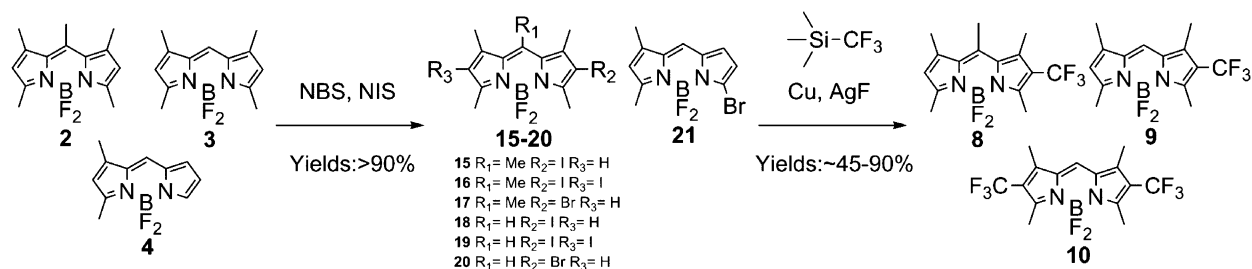
| Educt     | Product                  | New Substituent  | Position   | Yield [%] |
|-----------|--------------------------|------------------|------------|-----------|
| <b>24</b> | <b>7</b> <sup>[a]</sup>  | F                | $\alpha$   | 10        |
| <b>23</b> | <b>6</b> <sup>[a]</sup>  | F                | $\beta$    | 6         |
| <b>22</b> | <b>5</b> <sup>[a]</sup>  | F                | $\beta$    | 3         |
| <b>18</b> | <b>9</b> <sup>[b]</sup>  | $\text{CF}_3$    | $\beta$    | 93        |
| <b>19</b> | <b>10</b> <sup>[b]</sup> | 2x $\text{CF}_3$ | 2x $\beta$ | 81        |
| <b>15</b> | <b>8</b> <sup>[b]</sup>  | $\text{CF}_3$    | $\beta$    | 45        |

[a] Selectfluor,  $\text{Pd}(\text{terpy})\text{MeCN}$ , terpy,  $\text{KHF}_2$ , NaF, MeCN,  $40^\circ\text{C}$ , 15 h.  
[b]  $\text{AgF}$ ,  $\text{Me}_3\text{SiCF}_3$ , Cu, THF, RT, 12 h.

from Möller et al.<sup>[26]</sup> the reaction involves in situ generated “ $\text{CuCF}_3$ ”, which then performs the nucleophilic substitution. The monoiodo BODIPY dyes **15** and **18**, and diiodo BODIPY dyes **16** and **19** were obtained by using N-iodosuccinimide (NIS; 1 equiv or 2 equiv) in  $\text{CH}_2\text{Cl}_2$  at room temperature.<sup>[32]</sup> These halogenated compounds **15**, **16**, **18**, and **19** were subsequently converted into trifluoromethylated compounds by using  $\text{AgF}$ , Cu, and the Ruppert–Prakash reagent in DMF at  $25^\circ\text{C}$  (Scheme 3). The yields of this reaction were high for the



**Scheme 2.** Pd-catalyzed fluorination of BODIPY dyes.



**Scheme 3.** Insertion of trifluoromethyl groups using the Ruppert–Prakash reagent.

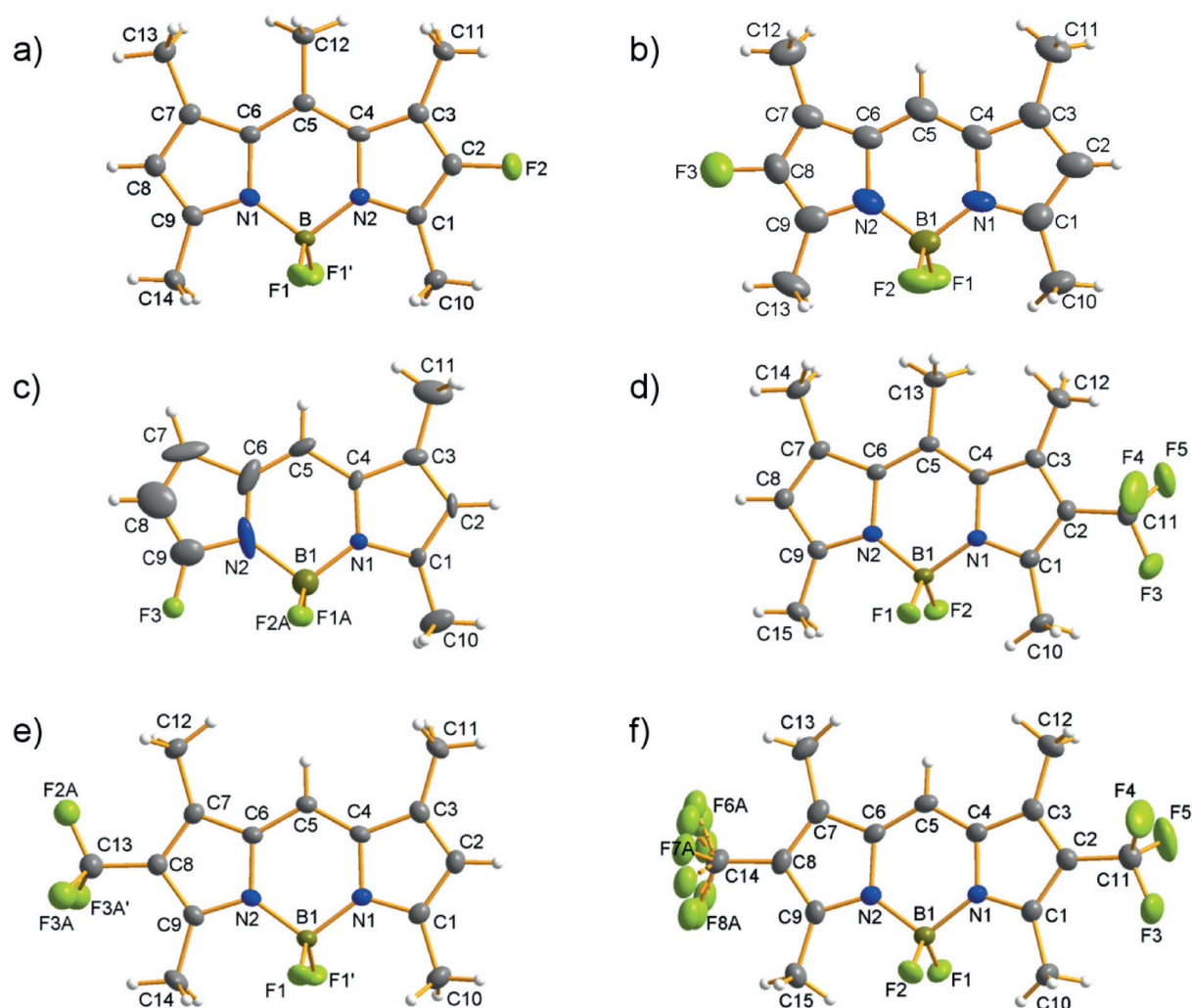


**Figure 3.** Collection of the crystallographic structures of compounds **5** (a), **6** (b), **7** (c), **8** (d), **9** (e) and **10** (f).<sup>[45]</sup> For further details, see the Supporting Information.

iodinated tetramethyl BODIPY dyes **18** and **19**. One or two trifluoromethyl groups can be easily introduced with high yields ( $\approx 80\text{--}90\%$ ). However, in case of the iodinated pentamethyl dyes, only compound **15** reacts under the mentioned conditions. The diiodinated pentamethyl derivative **16** reacted neither under these conditions nor at higher temperatures ( $80\text{--}100\text{ }^\circ\text{C}$ ). The same observation was made for the monobrominated tetramethyl, pentamethyl, and dimethyl derivatives **17**, **20**, and **21**; they turned out to be unreactive for these substitution reactions and the starting material could be recovered.

## 2.2 Spectroscopic Properties

The fluorescence properties of the synthesized BODIPY dyes **5–10** do not deviate largely from those of other compounds of this dye class.<sup>[10,11]</sup> They have narrow excitation and emission bands around 500 nm (Figure 4), high quantum yields ( $\Phi_{\text{fl}}$ ), and small Stokes shifts (Table 3). The introduction of  $\text{CF}_3$  groups at the  $\beta$  position (BODIPY **8**, **9**, and **10**) leads to blue-shifted electronic spectra compared with those of the parent compounds **2** and **3**. The largest shift of 17 nm was found for

| Table 3. Spectroscopic Properties of different BODIPY dyes. |                               |                              |   |  |                                   |                                  |   |
|---|-------------------------------|------------------------------|---|--|-----------------------------------|----------------------------------|---|
| Dye   | $\lambda_{\text{max}}$<br>abs | $\lambda_{\text{max}}$<br>em | $\tau_{\text{fl}}$<br>[ns] <sup>[a]</sup> | $\epsilon_{\text{max}}$<br>[ $\text{M}^{-1}\text{cm}^{-1}$ ] | $\Phi_{\text{fl}}$ <sup>[b]</sup> | ISC rate<br>[MHz] <sup>[c]</sup> | $\tau_{\text{avg}}$<br>[min] <sup>[d]</sup> |
| <b>4</b>  | 491                           | 504                          | 7.5                                       | 113000   | 0.93                              | 2.9                              | 1.5 (0.6)                                   |
| <b>7</b>  | 487                           | 510                          | 6.2                                       | 115000   | 0.96                              | 1.1                              | 3.8 (0.8)                                   |
| <b>3</b>  | 501                           | 507                          | 6.2                                       | 77000  | 1.0                               | 1.0                              | 1.0 (0.3)                                   |
| <b>6</b>  | 512                           | 521                          | 6.5                                       | 38000  | 1.0                               | 1.2                              | 3.5 (1.1)                                   |
| <b>9</b>  | 487                           | 498                          | 5.1                                       | 112000   | 1.0                               | 2.8                              | 1.3 (0.4)                                   |
| <b>10</b>   | 484                           | 492                          | 4.9                                       | 116000   | 1.0                               | 1.1                              | 3.0 (1.2)                                   |
| <b>2</b>  | 492                           | 505                          | 6.2                                       | 86000  | 0.79                              | 0.60                             | 0.6 (0.3)                                   |
| <b>5</b>  | 501                           | 514                          | 6.7                                       | 53000  | 0.82                              | 0.89                             | 1.7 (0.7)                                   |
| <b>8</b>  | 480                           | 501                          | 4.4                                       | 107000   | 0.83                              | 2.2                              | 1.0 (0.5)                                   |

[a] In MeCN. Standard error is  $\pm 0.1$  ns [b] Referenced to Fluorescein in 0.1 M KOH and Rhodamin 110 in basic EtOH. Standard error is 5–10%. [c] In  $\text{H}_2\text{O}$ . Standard error is  $\approx 30\%$ .<sup>[11,38]</sup> [d] Corrected with relative absorption cross-section at  $\lambda=488$  nm. Standard errors are given in parentheses.

the BODIPY **10**, which has two trifluoromethyl substituents. On the one hand, the influence of the electron-withdrawing  $\text{CF}_3$  groups is opposite to that of electron-donating substituents, such as in pyromethene 580 and 597,<sup>[33]</sup> and therefore not un-

expected at first glance. On the other hand, even electron-withdrawing groups such as bromide, chloride, or even fluoride (see below) in the  $\beta$  position lead to bathochromic shifts.<sup>[31]</sup> By contrast, a comparable hypsochromic effect is found in  $\beta$ -formyl-substituted BODIPY dyes.<sup>[34]</sup> The similarity of the unusual blueshift hints to some mesomeric effect of the  $\text{CF}_3$  groups, such as negative hyperconjugation.<sup>[35]</sup> In addition, a reduced fluorescence lifetime is a common feature upon their insertion, whereas the  $\Phi_{\text{fl}}$  values remain high, similar to the parent compounds. The concomitant reduction of the radiative lifetime results from the larger extinction coefficient, according to the Strickler–Berg relation, and may support the idea of extended conjugation including the  $\text{CF}_3$  groups.<sup>[36]</sup> In contrast, all monofluorinated dyes maintain high fluorescence lifetimes between 6.2 and 6.5 ns, corresponding to  $\Phi_{\text{fl}} > 80\%$ .  $\beta$ -fluorinated BODIPY dyes **5** and **6** exhibit 10 nm red-shifted electronic spectra compared with those of the parent dyes **2** ( $\lambda_{\text{abs}} = 492$ ,  $\lambda_{\text{em}} = 505$  nm) and **3** ( $\lambda_{\text{abs}} = 501$ ,  $\lambda_{\text{em}} = 507$  nm), whereas, similar to other halogenated BODIPYs,<sup>[31]</sup> but to a lesser extent, fluorination at the  $\alpha$  position in dye **7** leads to slightly shifted spectra of about 5 nm in comparison with that of BODIPY **4** ( $\lambda_{\text{abs}} = 491$ ,  $\lambda_{\text{em}} = 504$  nm). Also, the spectral width of the monofluorinated compounds, and subsequently, the extinction coefficient do not follow a general trend. Fluorination is known to distinctly alter the electronic properties of conjugated systems, for example with perfluorinated pentacene,<sup>[37]</sup> this might operate here as well, in a weakened manner. Although the influence of the respective substitution on the electronic spectra with respect to the starting material is minor compared with other substituents, the electronic spectra of **3** can overall be tuned by over almost 30 nm by insertion of F or  $\text{CF}_3$  groups (Figure 4).

For a more detailed characterization of the photophysical properties of the compounds, we performed FCS. This spectroscopic method allows the analysis of intersystem crossing (ISC) and the photostability of fluorescent dyes through observing their diffusional behavior.<sup>[11,38]</sup> Autocorrelation curves were recorded at various excitation intensities (Figure 5 a,b) and were subsequently fitted by using Equation (1):

$$g(\tau) = \frac{1}{\langle N \rangle} \cdot \left( \frac{1}{1 + \tau\tau_D} \right) \cdot \left( 1 + \frac{k_{23}}{k_{31}} \cdot \exp(-(k_{23} + k_{31}) \cdot \tau) \right) \quad (1)$$

The autocorrelation function,  $g(\tau)$ , is defined by the average particle number,  $\langle N \rangle$ , the diffusion time of the observed molecule,  $\tau_D$ , the ISC rate constant,  $k_{23}$ , and the triplet decay rate constant,  $k_{31}$ , which is the reciprocal of the triplet lifetime. The  $k_{31}$  value reflects the diffusion-controlled quenching of the triplet state by oxygen and is therefore similar for all measured compounds,<sup>[38]</sup> whereas the  $k_{23}$  value is directly related to the quantum yields for ISC. With the exception of the dimethyl BODIPY **4**, which exhibits a high ISC rate constant comparable to that of fluorescein,<sup>[11]</sup> monofluorination and trifluoromethylation only weakly enhances ISC, that is, maximally threefold higher rate constants are found with no clear correlation to the structure.

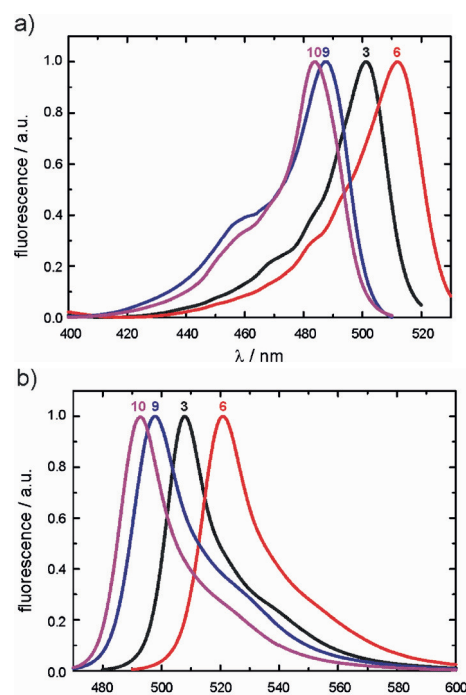


**Figure 4.** a) Excitation and b) emission spectra of tetramethyl BODIPY **3** (black) and its derivatives **6** (red), **9** (blue), and **10** (purple).

Information about the photostability can be drawn from the intensity-dependent diffusion time  $[\tau_D(I)]$ .<sup>[39]</sup> Photobleaching manifests itself in a shorting of  $\tau_D$  as fluorophores fade before leaving the observation volume (Figure 5c).<sup>[11]</sup> A Stern–Volmer-like plot allows for the assessment of the intensity-dependent rate constant  $k_{\text{bl}}$  for all bleaching processes, as long as saturation due to an exhaustive triplet population can be neglected (see the Supporting Information for saturation curves) [Eq. (2)]:<sup>[11,40]</sup>

$$\frac{\tau_D(0)}{\tau_D(I)} = 1 + k_{\text{bl}} \cdot \tau_D(0) \cdot I \quad (2)$$

Only compounds **2** and **3** and their monofluorinated derivatives **5** and **6** showed a change in diffusion time  $[\tau_D(I)]$  with increasing laser intensity. All other BODIPY dyes did not exhibit perceivable photobleaching. The resulting photobleaching rate ( $k_{\text{bl}}$ ) (Figure 5d) for the monofluorinated dye **6** is  $9.79 \cdot 10^{-5} \text{ cm}^2 (\text{kW } \mu\text{s})^{-1}$  in comparison with its parent dye **3** with a  $k_{\text{bl}}$  of  $6.69 \cdot 10^{-4} \text{ cm}^2 (\text{kW } \mu\text{s})^{-1}$ . The photobleaching rates for the compounds **2** and **5** are  $5.02 \cdot 10^{-4} \text{ cm}^2 (\text{kW } \mu\text{s})^{-1}$  and  $2.36 \cdot 10^{-4} \text{ cm}^2 (\text{kW } \mu\text{s})^{-1}$ , respectively. A comparison of the  $k_{\text{bl}}$  values of these four BODIPY dyes provides evidence that monofluorination of the fluorophore core results in slightly increased photostability, that is, a smaller  $k_{\text{bl}}$  value, by up to a factor of seven. The experimental finding of a stable diffusion time for all other compounds might already be interpreted as pronounced photostability. However, photophysical saturation, that is, limited number of photocycles, due to population of a long-lived triplet state during the transit time through observation of the volume, has to be discussed before this explana-

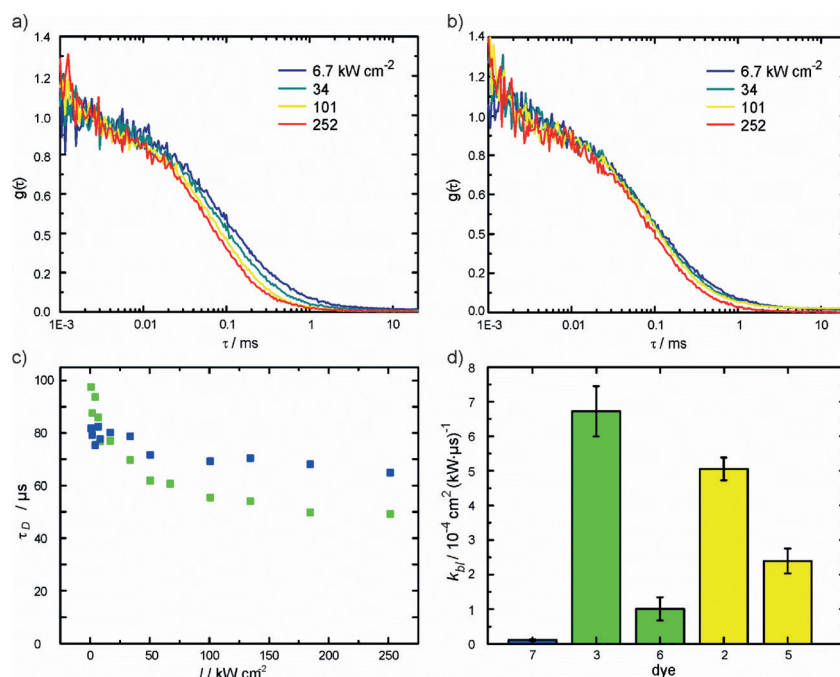


**Figure 5.** FCS analysis of photostability. Fluorescence autocorrelation function at different laser intensities for BODIPY dye 6 (a) and 7 (b). c) Intensity-dependent reduction of the apparent diffusion time  $t_D$  for BODIPY dye 6 (■) and 7 (■). d) Comparison of the  $k_{bi}$  values for BODIPY dyes 2, 3, 5, 6, and 7. For the color code for different methylation patterns see Figure 6.

tion becomes valid.<sup>[11]</sup> The steady-state population of the triplet state ( $\bar{T}$ ) is directly related to the determined  $k_{23}$  value at a certain excitation rate. Considering the similarity of the measured  $k_{23}$  values, that is, around 1 MHz for all monofluorinated derivatives 5–7, FCS hence supports a higher photostability than that of their parent substrates, at least for compounds 5 and 6, and an even higher photostability for the monofluorinated dye 7 can be anticipated. However, no conclusive interpretation for the trifluoromethylated BODIPY dyes 8–10, as well as for dye 4, can be made, as their  $\tau_D(I)$  do not change distinctly upon increasing laser intensities. Owing to the strong electronic saturation, resulting from a pronounced ISC, no Stern–Volmer-like plot can be obtained for the BODIPY dyes 4 and 8–10.

Subsequently, we used TIRF microscopy with a home-built setup to directly observe the photobleaching of the fluorinated BODIPY dyes and rhodamine 110, for comparison. TIRF microscopy is a convenient method to monitor the photobleaching of single fluorophores, regarding the time of their fluorescence at selected irradiation intensity.<sup>[41]</sup> Single molecules immobilized in polymethylmethacrylate (PMMA) were irradiated and imaged for 30 min at a laser intensity of  $30 \text{ W cm}^{-2}$  (Figure 6). At least three independently prepared samples were used to compensate for preparation inhomogeneities. In the recorded movies, we selected those molecules which were visible at the beginning of the experiment (Figure 6a) and analyzed the dwell time until their disappearance (Figure 6b). An empirical biexponential fit was applied to the normalized histogram of the residual molecules after the start of the experiment, obtained from 537 to 1187 trajectories (Figure 6d), and provided the average survival time ( $\tau_{avg}$ ) of the observed single molecules (Figure 6e, Table 3). The non-monoexponential

decay is attributed to the varying microenvironment of PMMA around the fluorophores and may be better described by multiexponential or stretched-exponential decay, which, however, does not provide additional mechanistic insights.<sup>[41a,c,42]</sup>

Monofluorinated derivatives 5–7 have considerably larger  $\tau_{avg}$  values than their parent compounds 2–4, respectively, thus confirming the results of our FCS experiments. It should be mentioned that the more intense excitation conditions in FCS than in TIRF (by at least a factor of 30) likely opens additional destruction pathways through higher excited states. A similar situation is met for the  $\text{CF}_3$  substituents.  $\tau_{avg}$  values of 8 and 9 are larger than those of their parent compounds 2 and 3, pointing to a stabilizing effect. In particular, the di(trifluoromethylated) compound 10 is distinctly more photostable than its parent tetramethyl BODIPY dye 3, by at least a factor of two or three, especially if one takes the stronger excitability at  $\lambda = 488 \text{ nm}$  into account (Figure 6f). In summary, we conclude that  $\text{CF}_3$  and F substituents increase the photostability of fluorescent dyes to a similar extent. Compounds 7 and 10 are therefore the most photostable fluorescent dyes studied here, due to the absence of destabilizing methyl groups, such as in compound 2, and despite being excited close to their absorption maxima. Roughly three million photocycles are estimated from TIRF imaging before photobleaching occurs (Figure 6f). Almost 25% of the molecules of compound 7 could be imaged for more than 5 min under continual irradiation (Figure 6c).

### 3. Conclusions

We successfully incorporated fluorine at several positions in the BODIPY scaffold. Monofluorination is preferentially

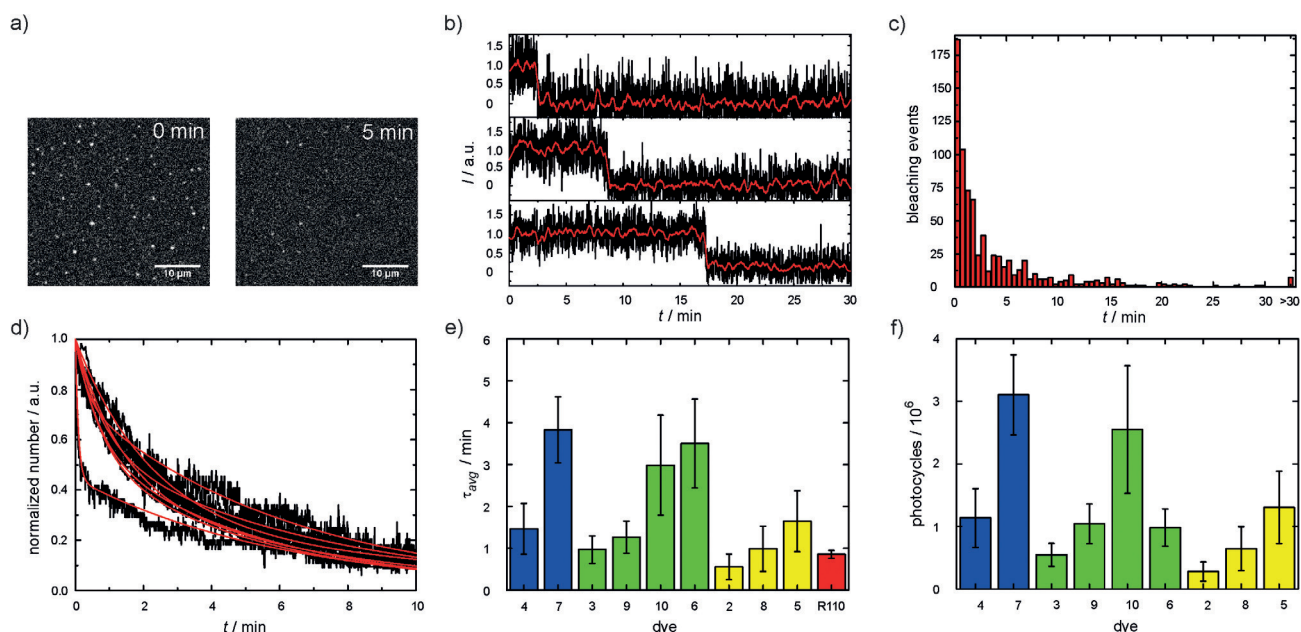


**Figure 6.** a) A  $39 \times 36 \mu\text{m}^2$  section of the TIRF image of BODIPY dye 7 at  $t = 0$  min (whole area:  $77 \times 77 \mu\text{m}^2$ ) and after 5 min. b) Representative time traces from three independent preparations. The red curve is obtained by averaging over five images. c) Bleaching histograms examples for BODIPY dye 7 recorded from three independent movies. d) Survival time distribution of BODIPY 7 from several independent movies, normalized to the observed molecules at the beginning. e) Average survival times  $\tau_{\text{avg}}$  for compounds 2–7 formed of 537–1187 molecules. Rhodamine 110 (R110) is used for comparison. f) Average photocycles before photobleaching on the basis of  $\tau_{\text{avg}}$ , obtained by taking different the extinction coefficient at  $\lambda_{\text{exc}} = 488$  nm into account.

achieved by using Selectfluor I at elevated temperatures, but the yields were generally not satisfying. We provided evidence that Selectfluor acts through SET under the described reaction conditions. Trifluoromethyl groups were introduced to the  $\beta$  position of the BODIPY core by using the nucleophilic Ruppert–Prakash reagent, thus complementing Togni’s reagent, which results in substitutions at the  $\alpha$  position.<sup>[14]</sup>

Furthermore, we examined the spectroscopic properties of these dyes and discovered that the absorption, excitation, and emission spectra only slightly differ from the parent BODIPY dyes. The measured fluorescence quantum yields ( $\Phi_{\text{f}}$ ) indicated that fluoro- and trifluoromethyl-substituted BODIPY dyes maintain high  $\Phi_{\text{f}}$  values. The introduction of  $\text{CF}_3$  moieties, however, distinctly decreased the fluorescence lifetimes. Both FCS and TIRF imaging experiments clearly revealed improved photostabilities upon monofluorination and the two-fold insertion of trifluoromethyl groups. For applications of the synthesized dyes in single-molecule chemistry and in life sciences, options for further modifications including those exploited for immobilization are available for these BODIPYs, due to unsubstituted or only methylated  $\alpha$  and  $\beta$  positions.<sup>[15a,24,43]</sup> We summarize that modification of the BODIPY core with Selectfluor I and the Ruppert–Prakash reagent was successful and gave higher yields than syntheses based on fluorinated pyrroles. The established trifluoromethylation and monofluorination schemes could be applied to aromatic fluorophores, for example, pyrenes and rylenes, for which we would expect higher yields than for the BODIPY scaffold.

## Experimental Section

### General

Reagents and solvents were used as purchased from Sigma–Aldrich, Merck, Acros Organics, and Carbolution Chemicals. The solvents used were dried using common laboratory methods. All air-sensitive reactions were carried out under an argon atmosphere. Analytical thin layer chromatography (TLC) was performed on silica gel 60 on PET-Foils (Fluka Analytik). Column chromatography was performed on a silica gel 60 (63–260  $\mu\text{m}$ ).

### NMR Spectroscopy

$^1\text{H}$ ,  $^{19}\text{F}$ , and  $^{13}\text{C}$  NMR spectra were recorded with a Bruker Avance 2 spectrometer (400, 376, or 100 MHz) at ambient temperature with reference to tetramethylsilane (TMS) or solvent standard with the chemical shifts recorded as  $\delta$  values in ppm units. Multiplicities are denoted as follows: s = singlet, d = doublet, t = triplet, and m = multiplet.

### UV/Vis and Fluorescence Spectroscopy

Absorption spectra were recorded using a commercial Jasco spectrophotometer (Jasco, V-650), and fluorescence emission and excitation spectra with a commercial Jasco spectrofluorometer (Jasco, FP-6500) at the micromolar concentrations, if not stated otherwise. Resolution was set to 1 nm.

### Time-Correlated Single-Photon Counting (TCSPC)

TCSPC measurements were performed with a home-built setup. Excitation was done with a pulsed laser diode (PicoQuant, LDH-PC-470,  $\lambda = 470$  nm; pulse width = 60–120 ps), which was controlled

by a diode laser driver unit (PDL 808 MC SEPIA, Pico-Quant). A single-photon avalanche detector (PDM 100ct SPAD, Micro Photon Devices) in combination with a photon-counting device (PicoHarp 300, PicoQuant) was used for detection. The overall instrumental response function was approximately 300 ps (full width at half maximum). Recorded data were analyzed using the SymPhoTime (Pico-Quant) and FluoroFit (PicoQuant) software.

### Fluorescence Correlation Spectroscopy

FCS measurements were performed using a custom-built setup, as described before.<sup>[11,44]</sup> A continuous-wave laser (Picarro, Soliton,  $\lambda = 488$  nm) with a beam diameter of 0.7 mm was used as the excitation source. The laser was coupled to an inverted microscope (Axiovert 200, Zeiss) and reflected by a dichroic mirror (495 DRLP resp. 555 DRLP Omega) into a water-immersion objective lens (PlanApo 63 $\times$ , NA 1.2 WI, Zeiss). The beam was focused onto a diffraction-limited spot above the cover slide (thickness  $0.17 \pm 0.01$  mm, Assistent). A drop of aqueous nanomolar dye solution placed on top of the cover slip served as the sample. Emitted fluorescence was collected by the same objective lens, passed through the dichroic mirror, and focused by the tube lens onto a 50  $\mu$ m pinhole. After filtering through a band pass filter (HQ 525/50 Analysentechnik), the light was split into two beams by a 50:50 beam splitter. Photons were detected by two avalanche photodiodes (SPCM-14-AQR, PerkinElmer Optoelectronics). The output of these modules was cross-correlated by a hardware correlator (FLEX 02-01D/C, Correlator.com). Laser power was varied from 10  $\mu$ W to 3 mW, corresponding to an intensity of 0.84–252 kW cm<sup>-2</sup>.

### Total Internal Reflection Microscopy

#### Immobilisation of Fluorophores

1 mL of a sonicated 20 mg mL<sup>-1</sup> PMMA solution in CHCl<sub>3</sub> was added to 1 mL of a micromolar concentrated dye solution in CHCl<sub>3</sub>. The resulting mixture was allowed to rest in the dark at ambient temperature overnight before it was diluted to nanomolar and sub-nanomolar concentrations of the dye. The final immobilization was performed by evaporation of the resulting nanomolar dye-PMMA solutions on glass coverslips (Menzel, Germany), and thereby producing a thin film of fixed dye molecules.

#### TIRF Imaging

The measurements were performed using a custom-built prism-based TIRF microscope.<sup>[38]</sup> A continuous-wave laser at  $\lambda_{\text{exc}} = 488$  nm (Picarro, Soliton) with a beam diameter of 0.7 mm was used as the excitation source. The laser was focused into a quartz prism (Suprasil1  $n_0 = 1.46$  at  $\lambda = 488$  nm; Melles Griot) by a plan-convex lens ( $f = 5$  cm) on top of an inverted microscope (Axiovert 200, Zeiss). The probe was placed under the prism between two cover slides (thickness  $0.17 \pm 0.01$  mm, Menzel) with water in between. The laser beam was totally reflected by the PMMA-water interface. The fluorescence was collected by an oil-immersion objective lens ( $\alpha$ -Plan-FLUAR 100 $\times$ , NA 1.45 Oil, Zeiss). The light was filtered by a dichroic mirror (495 DRLP, Omega) and a band pass filter (HQ 525/50, AHF Analysentechnik) and then detected by an EM-CCD camera (C9100-23B, Hamamatsu). The excitation power was  $\approx 30$  W cm<sup>-2</sup>. Image sequences (whole area:  $77 \times 77 \mu\text{m}^2$ ) were analyzed by using ImageJ Software (ImageJ 1.49d, Wayne Rasband, National Institute of Health, USA). Five (for Rhodamine110) or seven to nine movies (for compounds 2–10) of at least three inde-

pendent preparations with altogether 537 to 1187 molecules were recorded. Only those single molecules that were observed in the first frames were considered for analysis. This was done to exclude misinterpretations owing to blinking phenomena.

### Syntheses

General Procedure A: Me<sub>3</sub>SiCF<sub>3</sub> (1.2 equiv) was added to a well-stirred mixture of AgF (1.0 equiv) in 10 mL of DMF at room temperature. The mixture was stirred for 20 min and copper powder (1.5 equiv) was added. After stirring for 4 h, the formation of CuCF<sub>3</sub> was complete. The corresponding halogen-containing BODIPY dye (0.9 equiv) was added and the reaction mixture was stirred under at room temperature for 16 h. The mixture was filtered from the solid precipitate and evaporated under vacuum. The obtained crude product was purified by silica gel chromatography.

General Procedure B: Under an argon atmosphere, the BODIPY dye (1.0 equiv), bis(pinacolato)diboron (2.0 equiv) and potassium acetate (1.5 equiv) were dissolved in THF and the resulting solution was degassed. A catalytic amount of [1,1'-bis(diphenylphosphino)ferrocene] palladium(II) dichloride was added and the mixture was heated at 90 °C for 21 h. After cooling, the organic phase was washed with water and brine, dried over Na<sub>2</sub>SO<sub>4</sub>, and concentrated. The resulting residue was purified by flash chromatography to obtain the product.

2,4,4-Trifluoro-1,3,5,7,8-pentamethyl-4-bora-3a,4a-diaza-s-indacene (5): BODIPY 2 (50.0 mg, 0.19 mmol) was dissolved in dry methanol (40 mL) and heated to 60 °C. Selectfluor (100.0 mg, 0.28 mmol, 1.5 equiv) was then added in portions and stirred for 4 h. After cooling to room temperature, dichloromethane (30 mL) was added to the reaction mixture. The obtained suspension was filtered and the solvent was removed under reduced pressure. The crude product was purified by column chromatography (silica gel, *n*-hexane/dichloromethane 1:1) to give red needles (6.0 mg, 0.02 mmol, yield: 12%); <sup>1</sup>H NMR (CDCl<sub>3</sub>):  $\delta = 5.99$  (s, 1 H), 2.49 (s, 3 H, CH<sub>3</sub>), 2.45 (s, 3 H, CH<sub>3</sub>), 2.41 (s, 3 H, CH<sub>3</sub>), 2.34 (s, 3 H, CH<sub>3</sub>), 2.25 ppm (s, 3 H, CH<sub>3</sub>); <sup>13</sup>C NMR (CDCl<sub>3</sub>)  $\delta = 155.5, 142.2, 142.0, 138.8, 138.5, 132.5, 129.7, 121.4, 100.1$  (C–F), 17.3, 16.3, 14.5, 11.4, 10.2 ppm; <sup>19</sup>F NMR (CDCl<sub>3</sub>)  $\delta = -147.1$  (q, <sup>1</sup>J<sub>B,F</sub> = 32.7 Hz, 2 F, BF<sub>2</sub>), -163.4 (s, 1 F) ppm; HRMS (ESI): *m/z* calcd (%) for C<sub>14</sub>H<sub>17</sub>BF<sub>3</sub>N<sub>2</sub>: 281.14368 (M+H); found: 281.14338.

2,4,4-Trifluoro-1,3,5,7-tetramethyl-4-bora-3a,4a-diaza-s-indacene (6): Selectfluor (0.20 g, 0.56 mmol, 1.4 equiv) was slowly added to a solution of BODIPY dye 3 (0.10 g, 0.40 mmol) in absolute methanol (80 mL) at 60 °C. After stirring for 4 h, the reaction mixture was dissolved with CH<sub>2</sub>Cl<sub>2</sub> (30 mL), whereby a white solid precipitated. Then the suspension was filtered and the filtrate was concentrated under reduced pressure. Afterwards, the crude product was purified by column chromatography (silica gel, petroleum ether/dichloromethane 1.5:1) to give a red solid. (10.0 mg, 0.04 mmol, yield: 10%); <sup>1</sup>H NMR (CDCl<sub>3</sub>):  $\delta = 6.91$  (s, 1 H), 5.98 (s, 1 H), 2.46 (s, 3 H, CH<sub>3</sub>), 2.41 (s, 3 H, CH<sub>3</sub>), 2.17 (s, 3 H, CH<sub>3</sub>), 2.10 ppm (s, 3 H, CH<sub>3</sub>); <sup>13</sup>C NMR (CDCl<sub>3</sub>)  $\delta = 162.9, 158.7, 142.2, 142.2, 134.0, 120.8, 120.8, 119.2, 110.0, 14.7, 11.3, 10.5, 7.1$  ppm; <sup>19</sup>F NMR (CDCl<sub>3</sub>)  $\delta = -147.0$  (q, <sup>1</sup>J<sub>B,F</sub> = 32.7 Hz, 2 F, BF<sub>2</sub>), -162.4 ppm (s, 1 F); HRMS (ESI): *m/z* calcd (%) for C<sub>13</sub>H<sub>15</sub>BF<sub>3</sub>N<sub>2</sub>: 267.12803 (M+H), found: 267.12739.

4,4,5-Trifluoro-1,3-dimethyl-4-bora-3a,4a-diaza-s-indacene (7): Selectfluor (80.0 mg, 0.22 mmol, 1.0 equiv) was added to a solution of BODIPY 4 (50.0 mg, 0.22 mmol) in HPLC grade MeCN (25 mL) at 90 °C. After stirring for 2 h, additional Selectfluor (40.0 mg, 0.11 mmol, 0.5 equiv) was added. After stirring for an additional

6 h and cooling to room temperature, the solvent was removed under reduced pressure and the crude product was purified by column chromatography (silica gel, petroleum ether/dichloromethane 1:1) to give a red solid. (15.0 g, 0.06 mmol, yield 29%);  $^1\text{H NMR}$  ( $\text{CDCl}_3$ ):  $\delta = 7.01$  (d,  $^3J_{\text{H,F}} = 2.5$  Hz, 1H), 6.81 (t,  $^3J_{\text{H,H}} = 4.3$  Hz,  $^4J_{\text{H,F}} = 4.3$  Hz, 1H), 6.07 (s, 1H), 5.82 (t,  $^3J_{\text{H,F}} = 4.3$  Hz,  $^3J_{\text{H,H}} = 4.3$  Hz, 1H), 2.50 (s, 3H,  $\text{CH}_3$ ), 2.18 ppm (s, 3H,  $\text{CH}_3$ );  $^{13}\text{C NMR}$  ( $\text{CDCl}_3$ )  $\delta = 161.4$ , 160.5, 144.8, 135.3, 127.7, 125.3, 124.8, 120.8, 99.1, 15.0, 11.3 ppm;  $^{19}\text{F NMR}$  ( $\text{CDCl}_3$ )  $\delta = -106.2$  (t,  $^5J_{\text{F,F}} = 4.1$  Hz, 1 F),  $-147.3$  ppm (dq,  $^1J_{\text{B,F}} = 30.0$  Hz,  $^5J_{\text{F,F}} = 4.1$  Hz, 2 F,  $\text{BF}_2$ ); HRMS (ESI):  $m/z$  calcd (%) for  $\text{C}_{11}\text{H}_{11}\text{BF}_3\text{N}_2$ : 239.09673 (M+H); found: 239.09563.

4,4-Difluoro-1,3,5,7,8-pentamethyl-2-trifluoromethyl-4-bora-3a,4a-diaza-s-indacene (**8**): BODIPY dye **8** was synthesized according to General Procedure A and purified by column chromatography (silica gel, petroleum ether/dichloromethane 2:1) to give a red solid. (38.28 mg, 0.12 mmol, yield 45%);  $^1\text{H NMR}$  ( $\text{CDCl}_3$ ):  $\delta = 6.12$  (s, 1H), 2.57 (s, 3H,  $\text{CH}_3$ ), 2.55 (s, 3H,  $\text{CH}_3$ ), 2.49 (s, 3H,  $\text{CH}_3$ ), 2.42 (s, 3H,  $\text{CH}_3$ ), 2.38 ppm (s, 3H,  $\text{CH}_3$ );  $^{13}\text{C NMR}$  ( $\text{CDCl}_3$ )  $\delta = 159.0$ , 148.5, 144.8, 143.2, 136.8, 134.2, 130.4, 123.7, 122.9, 110.0, 17.8, 17.2, 14.8, 14.4, 13.1 ppm;  $^{19}\text{F NMR}$  ( $\text{CDCl}_3$ )  $\delta = -54.3$  (s, 3 F),  $-144.99$  ppm (q,  $^1J_{\text{B,F}} = 32.7$  Hz, 2 F,  $\text{BF}_2$ ); HRMS (ESI):  $m/z$  calcd (%) for  $\text{C}_{15}\text{H}_{17}\text{BF}_5\text{N}_2$ : 331.14049 (M+H); found: 331.14036.

4,4-Difluoro-1,3,5,7-tetramethyl-2-trifluoromethyl-4-bora-3a,4a-diaza-s-indacene (**9**): BODIPY dye **9** was synthesized according to General Procedure A and purified by column chromatography (silica gel, petroleum ether/dichloromethane 1:1) to give a red solid. (64.33 mg, 0.24 mmol, yield 93%);  $^1\text{H NMR}$  ( $\text{CDCl}_3$ ):  $\delta = 7.09$  (s, 1H), 6.11 (s, 1H), 2.55 (s, 3H,  $\text{CH}_3$ ), 2.51 (s, 3H,  $\text{CH}_3$ ), 2.27 (s, 3H,  $\text{CH}_3$ ), 2.23 ppm (s, 3H,  $\text{CH}_3$ );  $^{13}\text{C NMR}$  ( $\text{CDCl}_3$ )  $\delta = 162.9$ , 144.8, 135.7, 130.7, 130.7, 121.4, 121.2, 110.0, 57.1, 15.1, 13.1, 11.4, 10.2 ppm;  $^{19}\text{F NMR}$  ( $\text{CDCl}_3$ )  $\delta = 55.7$  (s, 3 F)  $-145.2$  ppm (q,  $^1J_{\text{B,F}} = 32.7$  Hz, 2 F,  $\text{BF}_2$ ); HRMS (ESI):  $m/z$  calcd (%) for  $\text{C}_{14}\text{H}_{13}\text{BF}_5\text{N}_2$ : 317.12484 (M+H); found: 317.12363.

4,4-Difluoro-1,3,5,7-tetramethyl-2,2-di(trifluoromethyl)-4-bora-3a,4a-diaza-s-indacene (**10**): BODIPY dye **10** was synthesized according to General Procedure A using 2.4 equiv of the trifluoromethylation reagents and purified by column chromatography (silica gel, petroleum ether/dichloromethane 2:1) to give a red solid. (62.24 mg, 0.20 mmol, yield 81%);  $^1\text{H NMR}$  ( $\text{CDCl}_3$ ):  $\delta = 7.28$  (s, 1H), 2.59 (s, 3H,  $\text{CH}_3$ ), 2.32 ppm (s, 3H,  $\text{CH}_3$ );  $^{13}\text{C NMR}$  ( $\text{CDCl}_3$ )  $\delta = 156.5$ , 144.5, 132.6, 124.7, 123.7, 122.0, 13.6, 10.4 ppm;  $^{19}\text{F NMR}$  ( $\text{CDCl}_3$ )  $\delta = -143.9$  (q,  $^1J_{\text{B,F}} = 32.7$  Hz, 2 F,  $\text{BF}_2$ ),  $-56.3$  ppm (s, 6 F); HRMS (ESI):  $m/z$  calcd (%) for  $\text{C}_{15}\text{H}_{14}\text{BF}_8\text{N}_2$ : 385.11222 (M+H); found: 385.11110.

4,4-Difluoro-1,3,5,7,8-pentamethyl-2-[4,4,5,5-tetramethyl-1,3,2-dioxaborolanyl]-4-bora-3a,4a-diaza-s-indacene (**22**): BODIPY dye **22** was synthesized according to General Procedure B and purified by column chromatography (silica gel, petroleum ether/dichloromethane 1:2) to give a red solid. (37.56 mg, 0.10 mmol, yield 33%);  $^1\text{H NMR}$  ( $\text{CDCl}_3$ ):  $\delta = 5.96$  (s, 1H), 2.63 (s, 3H,  $\text{CH}_3$ ), 2.50 (s, 3H,  $\text{CH}_3$ ), 2.47 (s, 3H,  $\text{CH}_3$ ), 2.43 (s, 3H,  $\text{CH}_3$ ), 2.29 (s, 3H,  $\text{CH}_3$ ), 1.24 ppm (s, 12H,  $\text{CH}_3$ );  $^{13}\text{C NMR}$  ( $\text{CDCl}_3$ )  $\delta = 153.9$ , 149.8, 141.9, 141.5, 133.0, 132.5, 121.7, 82.8, 29.7, 24.8, 17.4, 16.8, 16.7, 14.6, 14.4 ppm;  $^{19}\text{F NMR}$  ( $\text{CDCl}_3$ )  $\delta = -145.7$  ppm (q,  $^1J_{\text{B,F}} = 32.7$  Hz); HRMS (ESI):  $m/z$  calcd (%) for  $\text{C}_{20}\text{H}_{29}\text{B}_2\text{F}_2\text{N}_2\text{O}_2$ : 389.23832 (M+H); found: 389.23950.

4,4-Difluoro-1,3,5,7-tetramethyl-2-[4,4,5,5-tetramethyl-1,3,2-dioxaborolanyl]-4-bora-3a,4a-diaza-s-indacene (**23**): BODIPY dye **23** was synthesized according to General Procedure B and purified by column chromatography (silica gel, petroleum ether/dichloromethane 1:2) to give a red solid. (28.60 mg, 0.08 mmol, yield 25%);

$^1\text{H NMR}$  ( $\text{CDCl}_3$ ):  $\delta = 7.02$  (s, 1H), 5.99 (s, 1H), 2.63 (s, 3H,  $\text{CH}_3$ ), 2.46 (s, 3H,  $\text{CH}_3$ ), 2.33 (s, 3H,  $\text{CH}_3$ ), 2.17 (s, 3H,  $\text{CH}_3$ ), 1.23 ppm (s, 12H,  $\text{CH}_3$ );  $^{13}\text{C NMR}$  ( $\text{CDCl}_3$ )  $\delta = 164.1$ , 157.1, 150.4, 141.5, 134.0, 133.8, 120.1, 119.4, 82.8, 29.6, 24.9, 14.8, 14.6, 11.8, 11.2 ppm;  $^{19}\text{F NMR}$  ( $\text{CDCl}_3$ )  $\delta = -145.9$  ppm (q,  $^1J_{\text{B,F}} = 32.7$  Hz); HRMS (ESI):  $m/z$  calcd (%) for  $\text{C}_{19}\text{H}_{27}\text{B}_2\text{F}_2\text{N}_2\text{O}_2$ : 375.22266 (M+H); found: 375.22189.

4,4-Difluoro-1,3-dimethyl-2-[4,4,5,5-tetramethyl-1,3,2-dioxaborolanyl]-4-bora-3a,4a-diaza-s-indacene (**24**): BODIPY dye **24** was synthesized according to General Procedure B and purified by column chromatography (silica gel, petroleum ether/dichloromethane 1:2) to give a red solid. (18.52 mg, 0.05 mmol, yield 16%);  $^1\text{H NMR}$  ( $\text{CDCl}_3$ ):  $\delta = 7.26$  (d,  $^3J_{\text{H,H}} = 4.3$  Hz, 1H), 7.08 (s, 1H), 6.94 (d,  $^3J_{\text{H,H}} = 4.3$  Hz, 1H), 6.07 (s, 1H), 2.48 (s, 3H,  $\text{CH}_3$ ), 2.21 ppm (s, 3H,  $\text{CH}_3$ );  $^{19}\text{F NMR}$  ( $\text{CDCl}_3$ )  $\delta = -140.4$  ppm (q,  $^1J_{\text{B,F}} = 32.7$  Hz).

## Acknowledgements

Financial support from the German Science Foundation (DFG, JU650/3-1) is gratefully acknowledged.

**Keywords:** chromophores · dyes/pigments · fluorescence · fluorescence spectroscopy · photophysics

- [1] M. Wirtz, A. Grüter, F. Heib, V. Huch, J. Zapp, D.-P. Herten, M. Schmitt, G. Jung, *Methods and Applications in Fluorescence* **2015**, *3*, 044001.
- [2] a) N. Budisa, P. P. Pal, S. Alefelder, P. Birle, T. Krywcun, M. Rubini, W. Wenger, J. H. Bae, T. Steiner, *Biological Chemistry*, Vol. 385, **2004**, p. 191; b) P. P. Pal, J. H. Bae, M. K. Azim, P. Hess, R. Friedrich, R. Huber, L. Moroder, N. Budisa, *Biochemistry* **2005**, *44*, 3663–3672; c) M. H. J. Seifert, D. Ksiazek, M. K. Azim, P. Smialowski, N. Budisa, T. A. Holak, *J. Am. Chem. Soc.* **2002**, *124*, 7932–7942.
- [3] a) K. Mertens, D. Slaets, B. Lambert, M. Acou, F. De Vos, I. Goethals, *Eur. J. Nucl. Med. Mol. Imaging* **2010**, *37*, 2188–2193; b) J. S. Stehouwer, M. M. Goodman, *J. Labelled Compd. Radiopharm.* **2013**, *56*, 114–119.
- [4] B. E. Smart, *J. Fluorine Chem.* **2001**, *109*, 3–11.
- [5] A. E. Hoyt, B. C. Benicewicz, *J. Polym. Sci. Part A* **1990**, *28*, 3403–3415.
- [6] S. Mizukami, R. Takikawa, F. Sugihara, M. Shirakawa, K. Kikuchi, *Angew. Chem. Int. Ed.* **2009**, *48*, 3641–3643; *Angew. Chem.* **2009**, *121*, 3695–3697.
- [7] K. Müller, C. Faeh, F. Diederich, *Science* **2007**, *317*, 1881–1886.
- [8] a) H. Muramatsu, A. Okumura, K. Shibata, M. Matsui, *Chem. Ber.* **1994**, *127*, 1627–1632; b) Z. R. Woydziak, L. Fu, B. R. Peterson, *The Journal of Organic Chemistry* **2011**, *77*, 473–481; c) G. Y. Mitronova, V. N. Belov, M. L. Bossi, C. A. Wurm, L. Meyer, R. Medda, G. Moneron, S. Bretschneider, C. Eggeling, S. Jakobs, S. W. Hell, *Chem. Eur. J.* **2010**, *16*, 4477–4488.
- [9] a) T. Cordes, A. Maiser, C. Steinhauer, L. Schermelleh, P. Tinnefeld, *Phys. Chem. Chem. Phys.* **2011**, *13*, 6699–6709; b) J. H. M. van der Velde, J. Oelerich, J. Huang, J. H. Smit, M. Hiermaier, E. Ploetz, A. Herrmann, G. Roelfes, T. Cordes, *J. Phys. Chem. Lett.* **2014**, *5*, 3792–3798.
- [10] a) A. Loudet, K. Burgess, *Chem. Rev.* **2007**, *107*, 4891–4932; b) G. Ulrich, R. Ziessel, A. Harriman, *Angew. Chem. Int. Ed.* **2008**, *47*, 1184–1201; *Angew. Chem.* **2008**, *120*, 1202–1219; c) A. C. Benniston, G. Copley, *Phys. Chem. Chem. Phys.* **2009**, *11*, 4124–4131.
- [11] B. Hinkeldey, A. Schmitt, G. Jung, *ChemPhysChem* **2008**, *9*, 2019–2027.
- [12] a) H. Kobayashi, M. Ogawa, R. Alford, P. L. Choyke, Y. Urano, *Chem. Rev.* **2010**, *110*, 2620–2640; b) S. Suzuki, M. Kozaki, K. Nozaki, K. Okada, *J. Photochem. Photobiol. C* **2011**, *12*, 269–292; c) N. Boens, V. Leen, W. Dehaen, *Chem. Soc. Rev.* **2012**, *41*, 1130–1172; d) R. Ziessel, G. Ulrich, A. Harriman, *New J. Chem.* **2007**, *31*, 496–501.
- [13] a) K. Umezawa, A. Matsui, Y. Nakamura, D. Citterio, K. Suzuki, *Chem. Eur. J.* **2009**, *15*, 1096–1106; b) L. Li, B. Nguyen, K. Burgess, *Bioorg. Med. Chemistry Letters* **2008**, *18*, 3112–3116; c) S. G. Awuah, J. Polreis, V. Biradar, Y. You, *Org. Lett.* **2011**, *13*, 3884–3887; d) L. N. Sobenina, O. V. Petrova, K. B. Petruschenko, I. A. Ushakov, A. I. Mikhaleva, R. Meallet-Renault, B. A. Trofimov, *Eur. J. Org. Chem.* **2013**, 4107–4118; e) L. N. Sobenina,

- na, A. M. Vasil'tsov, O. V. Petrova, K. B. Petrusenko, I. A. Ushakov, G. Clavier, R. Meallet-Renault, A. I. Mikhaleva, B. A. Trofimov, *Org. Lett.* **2011**, *13*, 2524–2527.
- [14] N. Santschi, J. Cvengroš, C. Matthey, E. Otth, A. Togni, *Eur. J. Org. Chem.* **2014**, *2014*, 6371–6375.
- [15] a) A. Rybina, C. Lang, M. Wirtz, K. Größmayer, A. Kurz, F. Maier, A. Schmitt, O. Trapp, G. Jung, D.-P. Hertel, *Angew. Chem. Int. Ed.* **2013**, *52*, 6322–6325; *Angew. Chem.* **2013**, *125*, 6445–6449; b) M. Wirtz, A. Gruter, P. Rebmann, T. Dier, D. A. Volmer, V. Huch, G. Jung, *Chem. Commun.* **2014**, *50*, 12694–12697.
- [16] a) P. T. Nyffeler, S. G. Durón, M. D. Burkart, S. P. Vincent, C.-H. Wong, *Angew. Chem. Int. Ed.* **2005**, *44*, 192–212; *Angew. Chem.* **2005**, *117*, 196–217; b) X. Liu, C. Xu, M. Wang, Q. Liu, *Chem. Rev.* **2015**, *115*, 683–730.
- [17] W. J. Middleton, *J. Org. Chem.* **1975**, *40*, 574–578.
- [18] H. Hayashi, H. Sonoda, K. Fukumura, T. Nagata, *Chem. Commun.* **2002**, 1618–1619.
- [19] G. S. Lal, G. P. Pez, R. J. Pesaresi, F. M. Prozonc, H. Cheng, *The Journal of Organic Chemistry* **1999**, *64*, 7048–7054.
- [20] P. Kirsch, *Modern Fluoroorganic Chemistry*, 2nd Ed., Wiley-VCH, Weinheim, **2013**.
- [21] G. K. S. Prakash, M. Mandal, *J. Fluorine Chem.* **2001**, *112*, 123–131.
- [22] J. Joubert, S. Roussel, C. Christophe, T. Billard, B. R. Langlois, T. Vidal, *Angew. Chem. Int. Ed.* **2003**, *42*, 3133–3136; *Angew. Chem.* **2003**, *115*, 3241–3244.
- [23] M. S. Wiehn, E. V. Vinogradova, A. Togni, *J. Fluorine Chem.* **2010**, *131*, 951–957.
- [24] M. Sekiya, K. Umezawa, A. Sato, D. Citterio, K. Suzuki, *Chem. Commun.* **2009**, 3047–3049.
- [25] A. R. Mazzotti, M. G. Campbell, P. Tang, J. M. Murphy, T. Ritter, *J. Am. Chem. Soc.* **2013**, *135*, 14012–14015.
- [26] M. M. Kremlev, A. I. Mushta, W. Tyrta, Y. L. Yagupolskii, D. Naumann, A. Möller, *J. Fluorine Chem.* **2012**, *133*, 67–71.
- [27] R. E. Banks, *J. Fluorine Chem.* **1998**, *87*, 1–17.
- [28] A. B. Nepomnyashchii, A. J. Bard, *Acc. Chem. Res.* **2012**, *45*, 1844–1853.
- [29] S. P. Vincent, M. D. Burkart, C.-Y. Tsai, Z. Zhang, C.-H. Wong, *The Journal of Organic Chemistry* **1999**, *64*, 5264–5279.
- [30] X. Zhou, C. Yu, Z. Feng, Y. Yu, J. Wang, E. Hao, Y. Wei, X. Mu, L. Jiao, *Org. Lett.* **2015**, *17*, 4632–4635.
- [31] a) L. Jiao, W. Pang, J. Zhou, Y. Wei, X. Mu, G. Bai, E. Hao, *The Journal of Organic Chemistry* **2011**, *76*, 9988–9996; b) G. Duran-Sampedro, A. R. Agarrabeitia, I. Garcia-Moreno, A. Costela, J. Bañuelos, T. Arbeloa, I. López Arbeloa, J. L. Chiara, M. J. Ortiz, *Eur. J. Org. Chem.* **2012**, *2012*, 6335–6350.
- [32] H. Maeda, Y. Nishimura, S. Hiroto, H. Shinokubo, *Dalton Trans.* **2013**, *42*, 15885–15888.
- [33] J. H. Boyer, A. M. Haag, G. Sathyamoorthi, M.-L. Soong, K. Thangaraj, T. G. Pavlopoulos, *Heteroat. Chem.* **1993**, *4*, 39–49.
- [34] a) L. Jiao, C. Yu, J. Li, Z. Wang, M. Wu, E. Hao, *The Journal of Organic Chemistry* **2009**, *74*, 7525–7528; b) C. Yu, L. Jiao, H. Yin, J. Zhou, W. Pang, Y. Wu, Z. Wang, G. Yang, E. Hao, *Eur. J. Org. Chem.* **2011**, *2011*, 5460–5468.
- [35] C. M. R. Volla, A. Das, I. Atodiresei, M. Rueping, *Chem. Commun.* **2014**, *50*, 7889–7892.
- [36] S. J. Strickler, R. A. Berg, *The Journal of Chemical Physics* **1962**, *37*, 814–822.
- [37] M. C. R. Delgado, K. R. Pigg, D. A. da Silva Filho, N. E. Gruhn, Y. Sakamoto, T. Suzuki, R. M. Osuna, J. Casado, V. Hernández, J. T. L. Navarrete, N. G. Martinelli, J. Cornil, R. S. Sánchez-Carrera, V. Coropceanu, J.-L. Brédas, *J. Am. Chem. Soc.* **2009**, *131*, 1502–1512.
- [38] J. Widengren, U. Mets, R. Rigler, *J. Phys. Chem.* **1995**, *99*, 13368–13379.
- [39] C. Egeling, J. Widengren, R. Rigler, C. A. M. Seidel, *Anal. Chem.* **1998**, *70*, 2651–2659.
- [40] a) B. Finkler, C. Spies, M. Vester, F. Walte, K. Omlor, I. Riemann, M. Zimmer, F. Stracke, M. Gerhards, G. Jung, *Photochem. Photobiol. Sci.* **2014**, *13*, 548–562; b) S. Veetil, N. Budisa, G. Jung, *Biophys. Chem.* **2008**, *136*, 38–43.
- [41] a) R. Zondervan, F. Kulzer, M. A. Kol'chenk, M. Orrit, *J. Phys. Chem. A* **2004**, *108*, 1657–1665; b) J. W. Gilliland, K. Yokoyama, W. T. Yip, *Chem. Mater.* **2005**, *17*, 6702–6712; c) C. Julien, A. Débarre, D. Nutarelli, A. Richard, P. Tchénio, *J. Phys. Chem. B* **2005**, *109*, 23145–23153; d) T. Cordes, J. Vogelsang, M. Anaya, C. Spagnuolo, A. Gietl, W. Summerer, A. Herrmann, K. Müllen, P. Tinnefeld, *J. Am. Chem. Soc.* **2010**, *132*, 2404–2409; e) J. Vogelsang, R. Kasper, C. Steinhauer, B. Person, M. Heilemann, M. Sauer, P. Tinnefeld, *Angew. Chem. Int. Ed.* **2008**, *47*, 5465–5469; *Angew. Chem.* **2008**, *120*, 5545–5550.
- [42] a) J. Hernando, M. van der Schaaf, E. M. H. P. van Dijk, M. Sauer, M. F. García-Parajó, N. F. van Hulst, *J. Phys. Chem. A* **2003**, *107*, 43–52; b) F. Vargas, O. Hollricher, O. Marti, G. de Schaetzen, G. Tarrach, *The Journal of Chemical Physics* **2002**, *117*, 866–871.
- [43] a) T. Rohand, W. Qin, N. Boens, W. Dehaen, *Eur. J. Org. Chem.* **2006**, *2006*, 4658–4663; b) C. Lang, U. Gartner, O. Trapp, *Chem. Commun.* **2011**, *47*, 391–393; c) M. J. Spallek, G. Storch, O. Trapp, *Eur. J. Org. Chem.* **2012**, *2012*, 3929–3945.
- [44] W. P. Ambrose, P. M. Goodwin, J. P. Nolan, *Cytometry* **1999**, *36*, 224–231.
- [45] CCDC 1048472, 1048473, 1048474, 1048475, 1048476, and 1442574 contain the supplementary crystallographic data for this paper. These data are provided free of charge by The Cambridge Crystallographic Data Centre.

Manuscript received: October 3, 2015

Revised: November 25, 2015

Accepted Article published: December 2, 2015

Final Article published: December 23, 2015